NaSTech
JOURNAL OF NATURAL SCIENCES AND TECHNOLOGIES
2022, 1(1), 113-123, DOI: 10.5281/zenodo.7319331

MOLECULAR STRUCTURE, NBO AND TD-DFT ANALYSIS OF 4-METHYL-3-FURALDEHYDE BASED ON DFT CALCULATIONS

Nihal KUŞ

Department of Physics, Science Faculty, Eskisehir Technical University, 26470, Eskisehir, Turkey

ABSTRACT

In this study, molecular structure of 4-methyl-3-furaldehyde (4M3F) was analyzed using density functional theory (DFT) with level of B3LYP/6-311G++(d,p). As a result of the scanning of the CCC=O dihedral angle, two conformers (trans and cis) were found at minimum energy and the *trans* was more stable than the *cis* at ca. 6.4 kJ mol-1.

Time dependent DFT (TD-DFT) calculations have been used to calculate the low-energy excited states energies and oscillator strengths. As a result of calculations, it was found that the highest transition probability and most effective oscillator strength were in the $S_0 \rightarrow S_3$ singlet state for both conformers. This excitation energy corresponds to 5.9 eV for the trans conformer, while it is around 5.6 eV for the cis conformer.

The change in electron density in bonding-antibonding orbitals and their interactions as well as stabilization energies *E(2)* and natural atomic charges were calculated by Natural Bond Orbital (NBO) analysis. Electronic properties were analyzed using HOMO and LUMO energies.

Keywords: Keywords: 4-methyl-3-furaldehyde, Time dependent DFT, Natural Bond Orbital (NBO) analysis

1. INTRODUCTION

Aldehydes are organic compounds with a carbonyl group in their structure and hydrogens attached to this group. They are called aldehydes because they can usually be obtained from the dehydrogenation of alcohols at high temperatures. Furans are an aromatic heterocyclic ring of five atoms and the Ring has one oxygen and four carbon atoms. Furan and its derivatives play an important role in the pharmaceutical and chemical industry. Furan and its derivatives, which are also widely used in medicine and chemistry, are also atmospheric pollutants and are produced as a result of burning forests (1, 2). Furans, known as one of the most toxic volatile substances (3-5), contain polychlorine, which is dangerous for all living things, and are found in a wide variety of furan derivatives. Investigation of the presence of toxic compounds such as reactive aldehydes in foods is very common and has been an important research topic. With the increasing importance of consumer protection and quality control, it has started to be investigated more. Spano et al. reported that there are furanic aldehydes in honey (6). It has also been found in popcorn (7).

Theoretical studies of 5-nitro-2-furaldehyde oxime molecule, which is a derivative of furaldehyde, were studied by Arivazhagan et al. Vibration spectra of the molecule were examined, HOMO-LUMO and NBO analyzes were made (8). In our previous study, the structure of the 3-Furaldehyde (3FA) molecule, which is one of the furan pollutants in the atmosphere, was investigated using matrix isolation experiments (9). The interest in the furan molecule has increased day by day and theoretical studies on its derivatives have continued. In our previous study, the structure of the 3-Furaldehyde (3FA) molecule, which is one of the furan pollutants in the atmosphere, was investigated using matrix isolation experiments. Photochemical reactions were observed for matrix-isolated 3FA upon irradiation with $\lambda >$ 234 nm and $\lambda >$ 200 nm.

In this study, the two conformers of 4M3F (shown in Figure 1) differ by the orientation of the aldehyde group were studied theoretically by density functional theory (DFT) and Natural bond orbital (NBO) methods. Low-energy excited states were calculated using the time-dependent DFT (TD-DFT) theory (TD-DFT).

2. THEORETICAL CALCULATIONS

4M3F calculations were performed using the DFT program in Gaussian 09 (10) and analysis at minimum energy was performed. All calculations were done using the 6-311++G(d,p) basis set. The three-parameter hybrid density function, designated B3LYP, includes Becke's gradient change correction (11) and Lee, Yang, and Parr (12). DFT scans of the potential energy surface (PES) were used to define the minimum energy geometries of the molecule (*trans* and *cis* forms). These scans were carried out by

incrementally increasing the dihedral angles (15 degree steps) that determine the rotations of the aldehyde groups and optimizing (with energy minimization) the values of all other parameters.
NBO analysis was performed using NBO 3.1 by applying the Gaussian 09 program (13). Using the second-order Fock matrix, *trans* and *cis*-4M3F dominant donor-acceptor orbital interactions were investigated and analyzed.

The TD Schrödinger equation results of low-energy singlet and triplet states were calculated at B3LYP/6-311++G(d,p) theory level as functions of internal rotation of the aldehyde group of cis and trans forms (14,15).

3. RESULTS AND DISCUSSION

The two different conformational energies in the minimum energy state were calculated using B3LYP level and 6-311++G(d,p) basis set. The geometries of the two conformers found, together with their adopted atomic numbers, are shown in Figure 1.

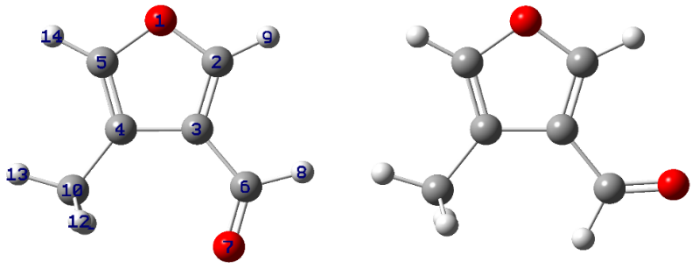

Figure 1. Conformers of 4M3F and Adopted Atom Numbering.

Calculations made for both trans and cis conformers were found to have a planar geometry and a C_s point group. Electronic energy difference (6.19 kJ mol^{-1} with ΔE+ZPV) was calculated 6.38 kJ mol^{-1} between the two conformers obtained due to the rotation of the aldehyde group. With this energy difference, the *trans* form is more stable than the *cis* form. The energy differences are given in Table 1. As a result of the calculations made about the 3FA molecule in the previous study, the *trans* form was found to be more stable than the cis form by 4.4 kJ mol^{-1}. Considering the zero point vibration energy correction, this value was calculated as 4.03 kJ mol^{-1} (9). Microwave spectrum study by Marstokk and Møllendal showed that the *trans* conformer of 3FA is at least 5 kJ mol^{-1} more stable than any other rotameric form of this molecule (16). Lunazzi et al. published that the minor conformer ratio should be approximately 11% at RT by studying 3FA conformations with dynamic NMR (17).

Table 1. Calculated electronic energies difference (with and without zero-point vibrational energy), Gibbs energy difference and dipole for *trans* and *cis* of 4M3F using B3LYP/6-311++g(d,p) level.

Energy	***Trans***	***cis***
ΔE (kJ mol^{-1})	0	6.38
ΔE(ZPV) (kJ mol^{-1})	0	6.19
ΔG (kJ mol^{-1})	0	5.94
dipole (debye)	2.52	3.57

By scanning the dihedral angles C−C−C=O (or C−C−O=H) in 15-degree steps, two conformers with the same energy value in both scans, called *trans* and *cis*, were obtained and presented in Figure 2. In the

figure, barrier energies and reverse energies are given. The calculated energy barrier for 4M3F-*trans* to 4M3F-*cis* was calculated as 39.8 kJ mol^{-1}. The reverse process is 33.4 kJ mol^{-1}.

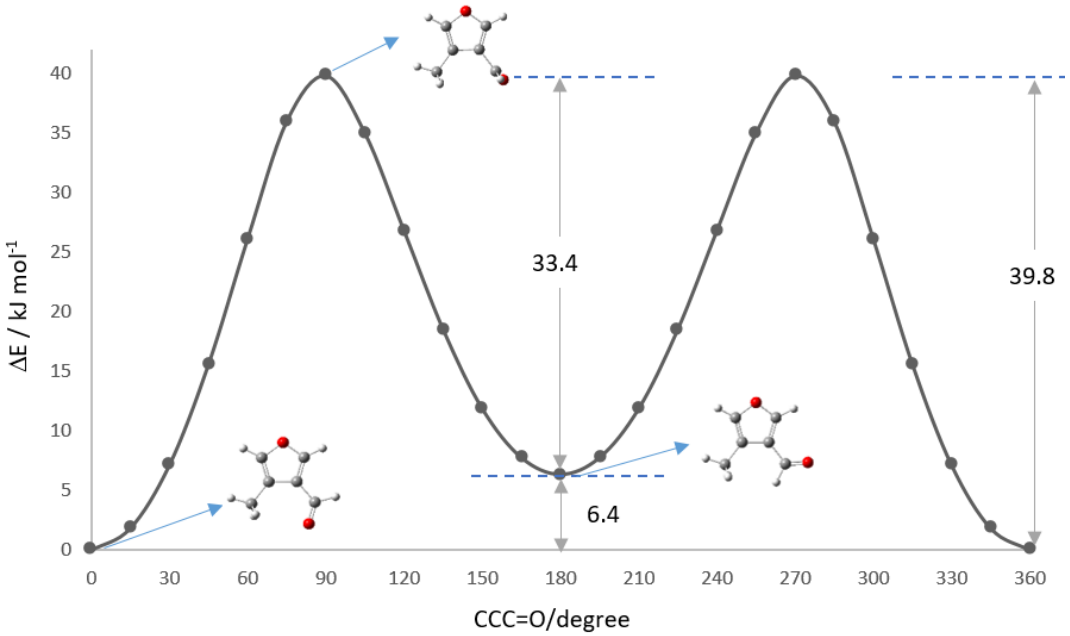

Figure 2. Potential energy profiles calculated by B3LYP/6-311++g(d,p) level for conformational interconversion in 4M3F (atom numbers are given in Fig. 1).

According to the value taken from the bottom of the potential well, the barrier energy calculated between the trans and cis form was 33.4 kJ mol^{-1}. (Fig. 2).

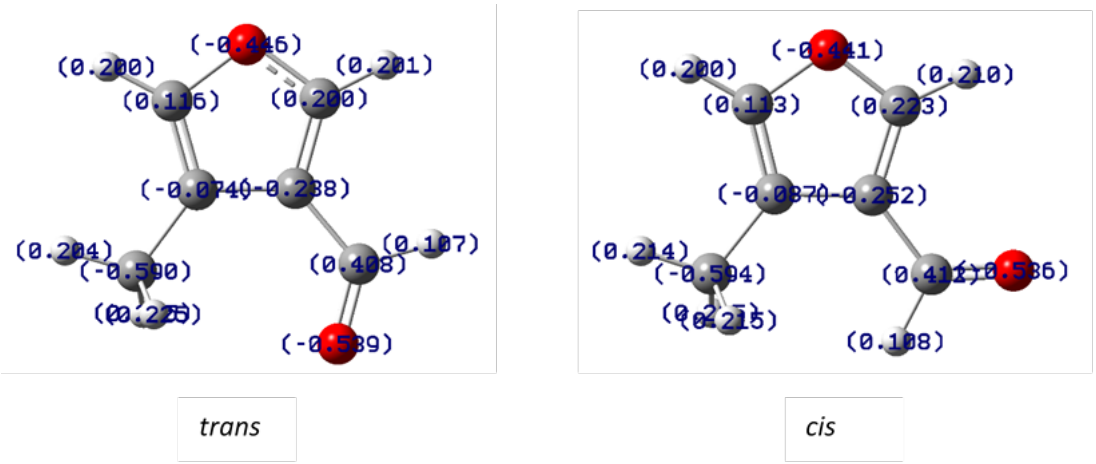

Figure 3. Natural atomic charges for trans and cis forms of 4M3F calculated by DFT/B3LYP/6-311++g(d,p) level of theory.

The NBO charges calculated for the two conformers were given in Figure 3. It is seen that the bond with the highest polarization for both the *trans* and *cis* forms of the charges indicated on the Figure 6 is the C3−H10 bond. For the trans form, the C3 charge is −0.288 *e*, the H10 charge is +0.408 *e*, while for the cis form, the corresponding charges for these atoms are calculated as -0.252 and +0.412 *e*. For both conformers, we can note that the C2−H9 bond is non-polarized. In this case, the charges for the trans form are +0.200 and +0.201 *e*, respectively, while for the cis form this value is +0.223 and +0.210 *e*.

Table 2. Orbitals, occupancy, coefficients, and hybridization for *trans* form of 4M3F, calculated using B3LYP/6-311++g(d,p) level.

trans	NBO	Occupancy Ratio	Coeficients (%)[a]		Hybridization[b]
			A	B	
Donor	π (C2−C3)	1.79070	45.64	54.36	0.6755p + 0.7373p
	π (C4−C5)	1.86963	48.48	51.52	0.69635p + 0.6893p
	L2(O1)	1.69387			p
	L1(O7)	1.98499			$sp^{0.69}$
	L2(O7)	1.88395			$spd^{2.75}$
Acceptor	π*(C4−C5)	0.23474	51.52	48.48	0.7178p - 0.6963p
	π*(C6=O7)	0.13253	66.94	33.06	0.8182p - 0.5749p
	π*(C2−C3)	0.30104	54.36	45.64	p
	RY1*(C6)	0.01152			$sp^{4.48}$
	σ*(C3−C6)	0.05428	46.78	53.22	$0.6840sp^{1.93}$ - $0.7295sp^{1.64}$
	σ*(C6−H8)	0.06659	42.82	57.18	$sp^{2.34}$ - s

[a] Percent contribution of each atom.
[b] Definition of hybrid orbitals.

The dipole interactions for both conformers were found to be related to the C=O bond with strong polarization (+0.408 and -0.589 *e* for *trans* form, and +0.412 and -0.586 *e* for *cis* form, respectively). Under these explanations, we can say that it is a proof that the bond that affects the lower energy of trans is the C4−H10 bond.

Table 3. Orbitals, occupancy, coefficients, and hybridization for *cis* form of 4M3F, calculated using B3LYP/6-311++g(d,p) level.

cis	NBO	Occupancy Ratio	Coeficients (%)[a]		Hybridization[b]
			A	B	
Donor	π (C2−C3)	1.78787	44.26	55.74	0.6653p + 0.7466p
	π (C4−C5)	1.87172	44.26	55.74	0.69635p + 0.6893p
	L2(O1)	1.69387			p
	L1(O7)	1.68785			$sp^{0.68}$
	L2(O7)	1.88467			p
Acceptor	π*(C4−C5)	0.24962	51.17	48.83	0.7153p - 0.6988p
	π*(C6=O7)	0.12315	66.85	33.15	0.8176p - 0.5757p
	π*(C2−C3)	0.29488	55.74	44.26	p
	RY1*(C6)	0.01153		49.63	$sp^{4.48}$
	σ*(C3−C6)	0.05428	46.78	53.22	$0.6841sp^{1.93}$ - $0.7294sp^{1.65}$
	σ*(C6−H8)	0.06509	42.82	57.18	$sp^{2.32}$ – s

[a] Percent contribution of each atom.
[b] Definition of hybrid orbitals.

Calculated NBOs with significant orbital interactions are given in Tables 2 and 3 for the trans and cis forms, respectively. These tables also show the percentage of atomic orbitals on each atom obtained from the NBO polarization coefficients and 1-center lone pair (LP-nonbonding) NBOs consists of a

single normalized natural hybrid orbital (NHO). 2-centered NBOs (BD-bonded atoms) consist of normalized linear combinations and can form π and σ bonds. NBOs corresponding to each phase of the valence hybrids form anti-bonds and indicate with BD* (π* or σ*). Valence non-Lewis NBOs are a series of "Rydberg type" 1-centered NBOs and are identified by the label RY*.

Regarding the occupancy rates in the two conformers, it was found that the occupancy rate of the L2(O7) atom was highest in *trans* and *cis* forms. We have also proved here that there is a strong polarization on this atom. It was found that the O1 atom of the furan ring has the p character in both conformers. However, the polarization of the O1−C2 bond is greater in the *cis* form than in the *trans* form. In the O1−C5 bond, the polarization is greater in the *trans* form. Two hybrid orbitals have strong polarization that these gives the same result as explained above in natural atomic charges. The orbital interactions with the highest stabilization energies for both forms are given in Table 4 and plotted in Figure 3. The table also shows the percentage of bond-forming atomic orbitals in each atom, deduced from the NBO polarization coefficients for NBO orbitals.

Table 4. Donor and acceptor interactions and stabilization energies for NBO pairs results from calculated by the Fock matrix equation (Eq.1) for *trans* and cis forms of 4M3F[a].

4M3F	Pair	Donor NBO *(i)*	Acceptor NBO *(j)*	*E(2)* kJ mol^{-1}	e_j- e_i au	F_{ij} au
trans	A1	π (C2−C3)	π*(C4−C5)	16.81	0.31	0.065
	B1	π (C2−C3)	π*(C6=O7)	22.21	0.30	0.074
	C1	π (C4−C5)	π*(C2−C3)	14.72	0.29	0.061
	D1	L2(O1)	π*(C2−C3)	**31.22**	0.36	0.094
	E1	L2(O1)	π*(C4−C5)	21.63	0.38	0.082
	F1	L1(O7)	RY1*(C6)	13.71	1.82	0.141
	G1	L2(O7)	σ*(C3−C6)	17.00	0.73	0.101
	H1	L2(O7)	σ*(C6−H8)	22.92	0.62	0.108
cis	A2	π (C2−C3)	π*(C4−C5)	18.09	0.30	0.067
	B2	π (C2−C3)	π*(C6=O7)	20.70	0.29	0.071
	C2	π (C4−C5)	π*(C2−C3)	14.21	0.30	0.060
	D2	L2(O1)	π*(C2−C3)	**31.64**	0.36	0.096
	E2	L2(O1)	π*(C4−C5)	22.42	0.37	0.083
	F2	L1(O7)	RY1*(C6)	13.97	1.80	0.142
	G2	L2(O7)	σ*(C3−C6)	17.28	0.73	0.102
	H2	L2(O7)	σ*(C6−H8)	22.54	0.62	0.107

[a] See atom numbering in Figure 1. LP, lone electron pair orbital, Ry, Rydberg orbital.

As can be seen from the G and H pairs in Table 4, these bonds belong to the aldehyde group and form strong sigma bonds for both *trans* and *cis* forms. The calculated total stabilization energy associated with the main orbital interactions was found to be almost the same for both conformations (160.22 kJ mol^{-1} and 160.85 kJ mol^{-1} for *trans* and *cis* forms, respectively). It was found that the most important

contribution to the stabilization was due to the LP2(O1) → π*(C2−C3) NBO pairs. While this value was 31.22 kJ mol^{-1} for the *trans* form, it was calculated as 31.64 kJ mol^{-1} for the *cis* form.

The electron densities between the donor and acceptor orbitals depend on the Lewis and non-Lewis NBO orbitals. Non-Lewis extra valence Rydberg orbitals are also included in the calculations of the stabilization energies obtained from the NBO results. The Fock matrix equation given in *Eq.1* is used for calculate stabilization energy, which is obtained from the 2nd order delocalization energies (13).

$$E(2) = \Delta E_{ij} = q_i \frac{F_{ij}^2}{\varepsilon_j - \varepsilon_i} \qquad (Eq.1)$$

In the *eq.1*, the term given with F_{ij} represents the matrix elements between the i and j NBO orbitals. The energies of donors and acceptors are given as ε_i and ε_j, respectively, and q_i indicates the occupancy rate of the donor orbital.

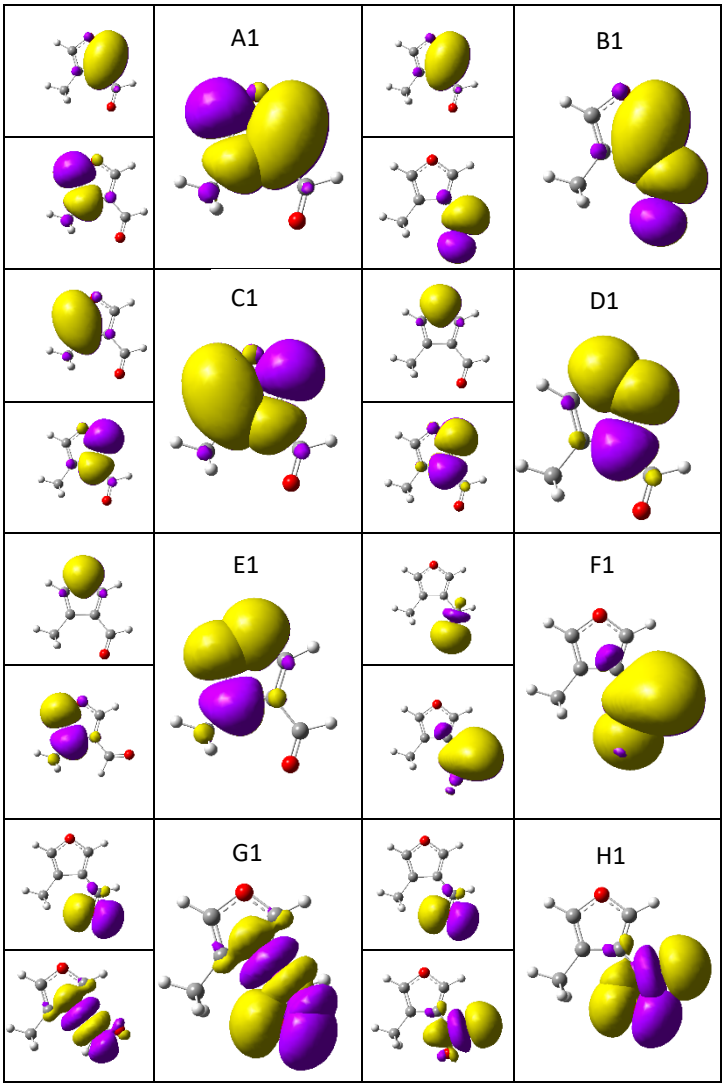

Fig. 4. NBOs electron density surfaces for *trans* of 4M3F calculated at the B3LYP/6-311++G(d,p) level of theory (see Table 2 for dominant interactions). The electron densities iso-values were chosen as 0.02 *e*. Negative and positive wave functions are shown with yellow and violet colors. Atom colors; red, O; gray, C; white, H.

The σ-type NBO interactions (G and H in Table 4), which contribute to the stabilization, are calculated with energies E(2), a sum of 39.92 kJ mol^{-1} for the *trans* form, a sum of 39.82 kJ mol^{-1} for the *cis* form, and they are found to be almost the same value. These interactions correlate with the electronic charge back-donation from the aldehyde oxygen lone electron pairs (specifically the p-type lone pair; LP2) to the C3-C6 bond and, in particular, to the C6-H8 aldehyde bond. This well-known back donation effect has been identified as the most significant effect leading to the observed elongation of the C-H bond attached to the carbonyl group and its reduced C-H stretching frequency as with aldehydes (18-20).
The same type of NBO interactions were observed in both forms of 4M3F, and the interaction with the highest energy was given with D1 and D2 pairs in Table 4. These interactions are of the trans and cis forms, respectively, and include the π-system of the molecule. The contribution of the D1 pair to the stabilization is the highest, and the total stabilization energy of the trans form (greater than 10% is taken into account) was calculated as 160.22 kJ mol^{-1}and the cis form as 160.85 kJ mol^{-1}. In this case, the *E(2)* energy of the *cis* is only 0.63 kJ mol^{-1} higher than *trans*.

Figure 4 and 5 show the pi orbital interactions in pairs A, B, C, and D. E and F lone electron pairs are oxygen and furan ring orbital interactions, while G and H pairs are sigma orbital interactions.

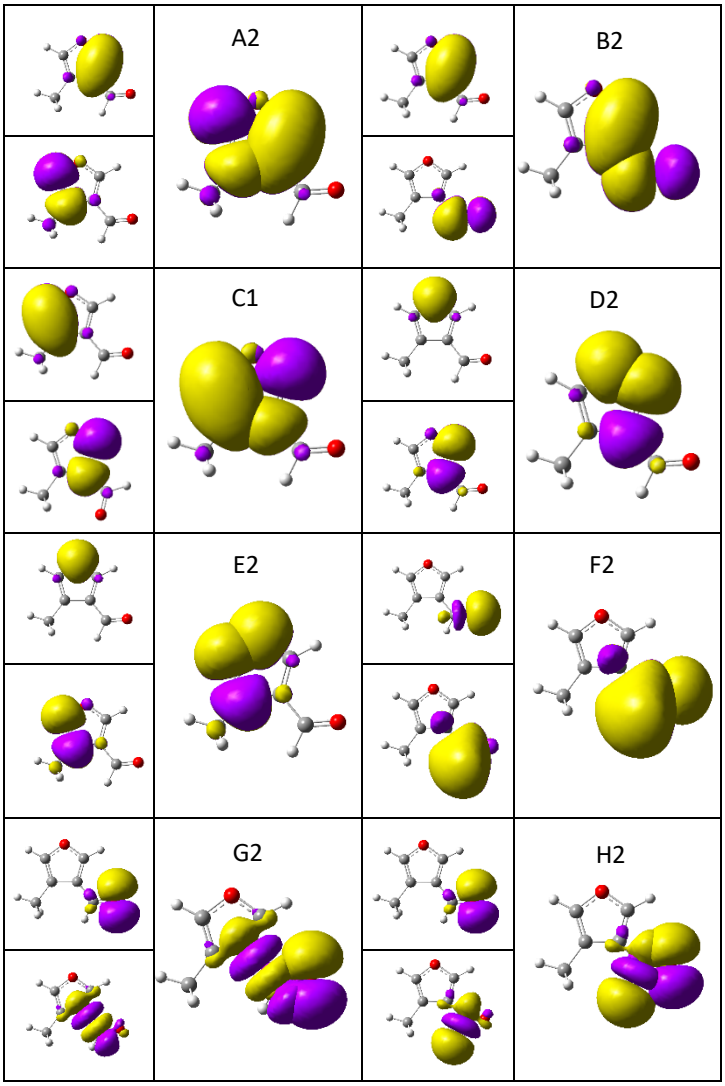

Fig.5. NBOs electron density surfaces for *cis* of 4M3F calculated at the B3LYP/6-311++G(d,p) level of theory (see Table 2 for dominant interactions). The electron densities iso-values were chosen as 0.02 *e*. Negative and positive wave functions are shown with yellow and violet colors. Atom colors; red, O; gray, C; white, H.

NaSTech
JOURNAL OF NATURAL SCIENCES AND TECHNOLOGIES
2022, 1(1), 113-123, DOI: 10.5281/zenodo.7319331

In the table 5, the percentage of electron density calculated by NBO method is given. The quality of the natural Lewis and non-Lewis structure is almost the same in both forms. Lewis and non-Lewis were calculated 56.93307 and 1.06693 for *trans*, 56.93715 and 1.06285 for *cis* forms of 4M3F. The NBO results also indicated the relatively important role of 170 Rydberg orbitals (NBOs 31-201) to valance non-Lewis orbitals (6 anti-bonds NBOs between 202-218) in the Lewis structure model for 4M3F.

Table 5. Total Lewis and non-Lewis occupancies (valence, core, and Rydberg shells) for *trans* and *cis* forms of 4M3F (e=1.60217646×10^{-19} C).

	trans	***cis***
Core	15.99392 (99.962% of 16)	15.99396 (99.962% of 16)
Valence Lewis	40.93915 (97.474% of 42)	40.94319 (97.484% of 42)
Total Lewis	**56.93307 (98.160% of 58)**	**56.93715 (98.168% of 58)**
Valance non-Lewis	0.96330 (1.661% of 58)	0.96103 (1.657% of 58)
Rydberg non-Lewis	0.10363 (0.179% of 58)	0.10182 (0.176% of 58)
Total non-Lewis	**1.06693 (1.840% of 58)**	**1.06285 (1.832% of 58)**

Table 6. Energy of Vertical Absorption (ΔE) and Oscillator Strength (*f*) of Trans and Cis Conformers of 3FA Calculated for their Ground State Equilibrium Geometries Using the TD-DFT Method at theB3LYP/6-311++G(d,p) Level.

***trans* – 4M3F**					***cis* – 4M3F**				
state	***type***	***E/ eV***	***E/ nm***	***f***	***state***	***type***	***E/ eV***	***E/ nm***	***f***
S_0		0			S_0		0.07		
S_1	n-π*	3.91	317.24	0.0002	S_1	n-π*	3.75	330.61	0.0001
S_2	π-π*	4.66	266.19	0.0373	S_2	π-π*	4.48	276.89	0.0372
S_3	**π-π***	**5.87**	**211.32**	**0.1542**	**S_3**	**π-π***	**5.61**	**221.02**	**0.1465**
S_4	π-π*	5.98	207.25	0.0000	S_4	π-π*	5.82	213.18	0.0002
S_5	π-π*	5.99	206.89	0.0007	S_5	π-π*	6.13	6.1263	0.0005
S_6	π-π*	6.05	204.78	0.0089	S_6	π-π*	6.19	200.22	0.1060

Table 6 summarizes the six calculated lowest excited singlet states of *trans* and *cis* forms of 4M3F resulting from TD-DFT calculations. It was observed that while the excitation energy was 5.98 eV (λ = 207.25 nm) in the S_4 state in the *trans* form, there was no oscillator power. A very low oscillator power indicates that the $S_0 \rightarrow S_1$ excitation is ineffective. The highest oscillator power is observed in the S_3 state in both *trans* (0.1542) and *cis* (0.1465) forms of 4M3F. In this case, we can say that $S_0 \rightarrow S_4$ excitation can be at the most effective level and changes in the molecular structure can be observed as a result of the excitation (λ >211). The potential energy graph of excited singlet states formed as a result of aldehyde group rotation is given in figure 6. As can be seen from the graph, the energies of the S_2 and S_3 states have increased in parallel with each other. According to the TD-DFT results obtained with the 105° rotation of the aldehyde group, it was found that the S_0+S_4 and S_0+S_5 singlet states were at the same energy. Likewise, S_0+S_5 and S_0+S_6 singlet barrier energies were found to be equal to each other as a result of rotation with an angle of 120° (Fig.6).

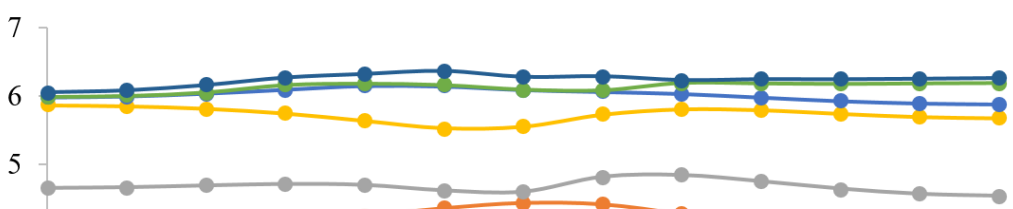

JOURNAL OF NATURAL SCIENCES AND TECHNOLOGIES
2022, 1(1), 113-123, DOI: 10.5281/zenodo.7319331

Fig. 6. Potential energy curves of the lowest excited singlets of 4M3F calculated using the theory level B3LYP/6-311++G(d,p) as a result of rotation of aldehyde group.

While the S_1 singlet state exhibits minimum energy at two points (0 and 180°) in *trans* and *cis* form, as in the ground state, the first minimum observed in the S_2 singlet state was determined when the aldehyde group was 90°. In the S_3 singlet state, the first minimum was obtained by rotation of the aldehyde group by 75 degrees, while in the S_4, S_5 and S_6 singlet states the trans form was still in the 0° state of the aldehyde group when ground state energies are added.

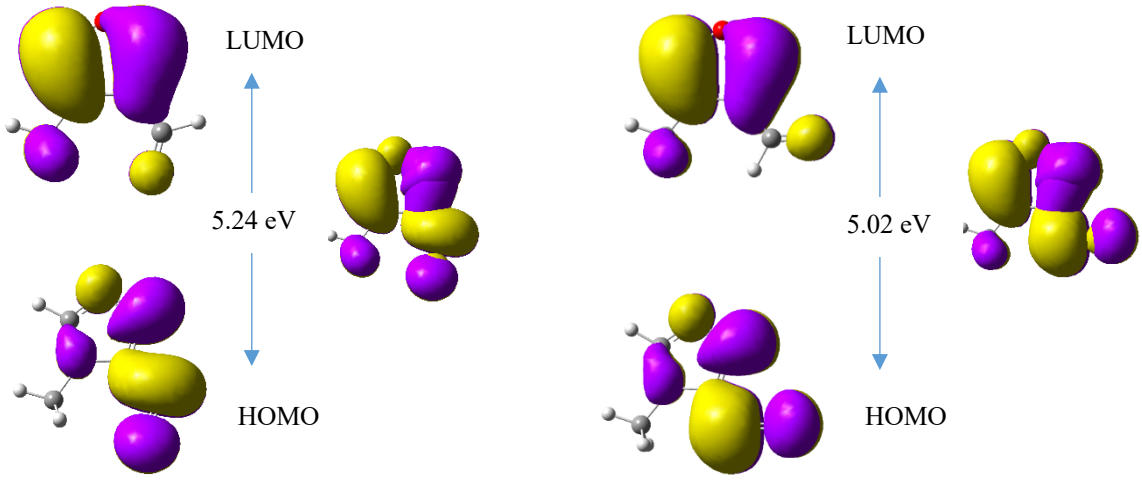

Fig. 7. Orbital schemes of HOMO-LUMO energy differences for *trans* and *cis* forms.

The electrons of covalently bonded molecules are assumed to reside in molecular orbitals formed by orbitals of atoms. Each of these orbitals has different steady-state energies. Filled orbitals are donors, vacant orbitals are acceptors. Shorter HOMO-LUMO gap indicate that the molecule has high reactivity (color: yellow is a positive value and purple is a negative value). The HOMO tends to donate the outermost orbital containing electrons, and these electrons act as an electron donor. On the other hand, LUMO refers to the orbital containing free sites to accept an innermost electron. The HOMO-LUMO energy difference was found to be 5.24 and 5.02 eV for *trans* and *cis* forms, respectively. The negative and positive density distributions of the HOMO and LUMO orbitals are given in Figure 7.

Electron density calculated for trans and cis are given with color codes and surface maps of molecular electrostatic potential (MEP) are shown in Fig. 8. The MEP map shows the Van der Waals surface for the *trans* and *cis* forms, and the approximate maximum distance that electron densities can reach is calculated on this surface.

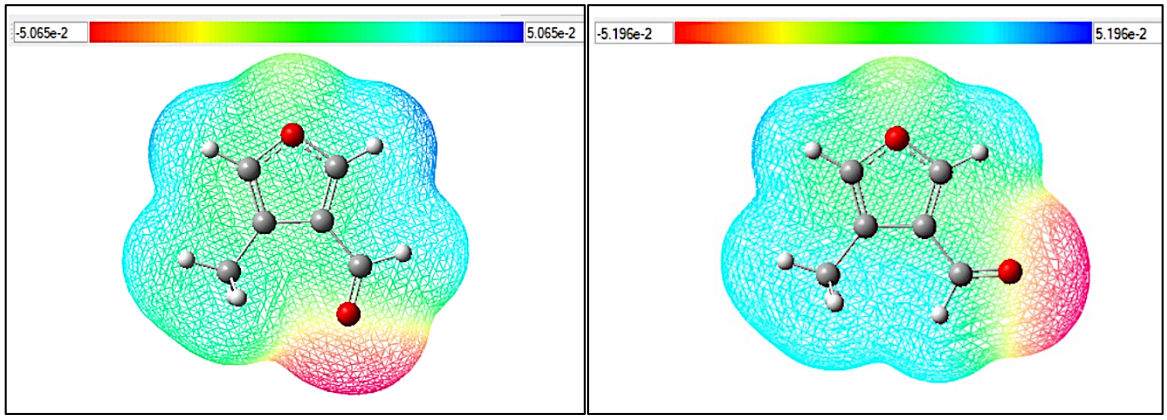

Fig. 8. MEP surface for *trans* and *cis* forms of 4M3F.

GaussView5 visualization program was used while drawing MEP surfaces of *trans* and *cis* conformers. MEP can be defined as the interaction energy between the unit positive charge and the charge distribution of the molecular system. Color coding system is used to define MEP. On the MEP map, the most negative potential (the region where the electron density is higher than the nucleus over the entire molecule) is shown in red, while blue is used to show the most positive potential (the region of partial positive charges) (21). These values are +5.065e-2 (max. red region) to -5.065e-2 (max. blue region) for the transform and +5.196e-2 (max. red region) to -5.196e-2 (max. blue region) for the cis form. The map showed that for the *trans* and *cis* forms, (red region, electrophilic attack) concentrated around the OH aldehyde group, while the maximum positive electrostatic potential (blue region, nucleophilic attack) increased around the hydrogen atoms of the furan ring.

4. CONCLUSIONS

The conformers of 4M3F were calculated in the ground electronic state using DFT/B3LYP/6-311++g(d,p) level of theory. Trans form was more stable than the cis *ca.* 6.19 kJ mol^{-1} taking account zero point vibration energy. The dipole interactions for the trans and cis forms were found to be with strong polarization of the C=O bond. Orbital interaction energies, electron density surfaces and hybridizations of 4M3F were determined using B3LYP/6-311++g(d,p) level using NBO method. The NBO pair that contributed the most to the stabilization energy was found to originate from the LP2(O1) → π*(C2−C3) orbital interaction. The quality of the natural Lewis and non-Lewis structure is almost the same in both forms. The calculated six lowest excited singlet states of the trans and cis forms of 4M3F were obtained from TD-DFT calculations. The HOMO-LUMO energy gap was calculated for *trans* and *cis* forms. From the energy gap, it can be estimated that the mobility of the π electrons of the trans form is slightly greater than that of the cis form. According to the natural charge distribution on the atoms and the MEP map, the negative electrostatic potential region was observed around the oxygen atom attached to the aldehyde, while the positive potential region was observed around the hydrogen atoms for two conformers.

ACKNOWLEDGMENT

This work was supported by the Eskisehir Technical University Commission of Research Project under grant no: 22ADP074.

REFERENCES

[1] Yokelson, R. J.; Karl, T.; Artaxo, P.; Blake, D. R.; Christian, T. J.; Griffith, D. W. T.; Guenther, A.; Hao, W. M. Atmos. Chem. Phys. 2007, 7, 5175–5196.
[2] Karl, T. G.; Christian, T. J.; Yokelson, R. J.; Artaxo, P.; Hao, W. M.; Guenther, A. Atmos. Chem. Phys. 2007, 7, 5883–5897.
[3] Amaro, M. I.; Monasterios, M.; Avendan˜o, M.; Charris, J. J. J. Appl. Tox. 2009, 29, 36–41.
[4] Seawright, A. A.; Mattocks, A. R. Experientia 1973, 29, 1197–1200.
[5] Bell, J. U. Waste Manage. 2002, 22, 405–412.
[6] Spano, N.; Ciulu, M.; Floris, I.; Panzanelli, A.; Pilo, M. I.; Piu, P. C.; Salis, S.; Sanna, G. Talanta 2009, 78, 310–314.
[7] Park, D.; Maga, J. A. Food Chem. 2006, 99, 538–545.
[8] Arivazhagan, M; Jeyavijayan, S; Geethapriya, J. Spectrochim Acta A Mol Biomol Spectrosc. 2013, 104:14–25.
[9] Kuş, N; Reva, I and Fausto, R. The Journal of Physical Chemistry A 2010 114 (47), 12427-12436.
[10] Frisch M. J et al. Gaussian 09, Revision A.0.2. Gaussian Inc, Wallingford CT, 2009.
[11] Becke, A. D. Phys. ReV. A 1988, 38, 3098–3100.
[12] Lee, C. T.; Yang, W. T.; Parr, R. G. Phys. ReV. B 1988, 37, 785–789.
[13] Weinhold, F.; Landis, C. R. Valency and Bonding. A Natural Bond Orbital Donor-Acceptor PerspectiVe; Cambridge University Press: New York. 2005.
[14] Bauernschmitt, R.; Ahlrichs, R. Chem. Phys. Lett. 1996, 256, 454–464.
[15] Stratmann, R. E.; Scuseria, G. E.; Frisch, M. J. J. Chem. Phys.1998, 109, 8218–8224.
[16] Marstokk, K.-M.; Møllendal, H. Acta Chem. Scand. 1992, 46, 923–927.
[17] Lunazzi, L.; Placucci, G.; Macciantelli, D. Tetrahedron 1991, 47, 6427–6434.
[18] Fausto, R.; Batista de Carvalho, L. A. E.; Teixeira-Dias, J. J. C.; Ramos, M. N. J. Chem. Soc., Faraday Trans. 2 1989, 85, 1945–1962.
[19] McKean, D. C. Chem. Soc. ReV. 1978, 7, 399–422.
[20] Castiglioni, C.; Gussoni, M.; Zerbi, G. J. Chem. Phys. 1985, 82, 3534–3542.
[21] Cramer C.J. 2004. Essentials of Computational Chemistry: Theories and Models, Computational Chemistry, 596.